


RESEARCH ARTICLE

WILEY

Enhancing urban runoff modelling using water stable isotopes and ages in complex catchments

Aaron Smith¹ | Doerthe Tetzlaff^{1,2,3} | Christian Marx⁴  | Chris Soulsby^{2,3} 

¹IGB Leibniz Institute of Freshwater Ecology and Inland Fisheries Berlin, Berlin, Germany

²Geographisches Institut, Humboldt University Berlin, Berlin, Germany

³Northern Rivers Institute, School of Geosciences, University of Aberdeen, Aberdeen, UK

⁴Institute of Applied Geosciences, Technische Universität Berlin, Berlin, Germany

Correspondence

Aaron Smith, IGB Leibniz Institute of Freshwater Ecology and Inland Fisheries Berlin, Berlin, Germany.
Email: aaron.smith@igb-berlin.de

Funding information

Bundesministerium für Bildung und Forschung; Deutsche Forschungsgemeinschaft; Einstein Stiftung Berlin; Leverhulme Trust

Abstract

Increased urbanization, coupled with the projected impacts of climatic change, mandates further evaluation of the impact of urban development on water flow paths to guide sustainable land-use planning. Though the general urbanization impacts of increased storm runoff peaks and reduced baseflows are well known; how the complex, non-stationary interaction of the dominant water fluxes within dynamic urban water stores sustain streamflow regimes over longer periods of time is less well quantified. In particular, there is a challenge in how hydrological modelling should integrate the juxtaposition of rapid and slower flow pathways of the urban 'karst' landscape and different approaches need evaluation. In this context, we utilized hydrological and water stable isotope datasets within a modelling framework that combined the commonly used Hydrologic Engineering Center Hydrological Modelling System (HEC-HMS) urban runoff model along with a simple hydrological tracer module and transit time modelling to evaluate the spatial and temporal variation of water flow paths and ages within a heavily urbanized 217 km² catchment in Berlin, Germany. Deeper groundwater was the primary flow component in the upper reaches of the catchment within fewer urbanized regions, while the addition of wastewater effluent in the mid-reaches of the catchment was the dominant water supply to sustain baseflow in the lower main stem stream, with additional direct storm runoff and shallow subsurface contributions in the more urbanized lower reaches. Water ages from each modelling approach mirrored flow contributions and water age mixing potential in subsurface storage; with older average water and lower young water contributions in less urbanized sub-catchments and younger average water and higher young water contributions in more urbanized regions. The results from the first step towards more integrated tracer-aided hydrologic modelling tools for similar peri-urban catchments, given the potential limitations of simpler model frameworks. The results have broader implications for assessing the uncertainty in evaluating urban impacts on hydrological function under environmental change.

KEYWORDS

hydrological modelling, urban hydrology, water ages, water stable isotopes

This is an open access article under the terms of the [Creative Commons Attribution](https://creativecommons.org/licenses/by/4.0/) License, which permits use, distribution and reproduction in any medium, provided the original work is properly cited.

© 2023 The Authors. *Hydrological Processes* published by John Wiley & Sons Ltd.

1 | INTRODUCTION

With an increasing proportion of the global population living within high-density urban environments (currently >50%, United Nations, 2018) and the projected impact of climate change on built areas (Güneralp et al., 2015; Pang et al., 2022), there is a need for continual improvement of hydrological understanding to provide an evidence base for various stakeholders to make informed decisions about urban water resources. In particular, the need to maintain the provision of ecosystem services, such as drinking water supplies or in-stream flows, which can be dependent on urban groundwaters and surface waters (European Environment Agency, 2014; Turner et al., 2021), has increased the importance of evaluating the complex interactions between evolving urban landscapes and their sensitivity to hydrological change. While urban environments have been the focus of many hydrological modelling studies, these have traditionally focused on engineered drainage and stormwater management, with limited evaluation of ecohydrological fluxes in urban green spaces, which can comprise a significant proportion of urban landscapes (McGrane, 2016). Much of this limited evaluation is due to the inherent complexities of integrating the 'natural' and 'engineered' components of urban hydrological systems which have very different spatial patterns and temporal dynamics and thus limit the use of traditional modelling and analytical approaches (Fletcher et al., 2013). This has subsequently led to increasing focus in the recent years on characterizing the spatio-temporal heterogeneity of urban/rural landscape water interfaces in different geographical settings (e.g. Fidal & Kjeldsen, 2020). However, there remains a need to understand the interaction of artificial drainage (and wastewater effluents) and the more 'natural' hydrology – sustaining in-stream habitats and dry season groundwater recharge – of rural and urban green spaces. This research need is urgent given the rapid urban growth at a time of projected reductions in water availability in many areas due to climate change (Nguyen et al., 2010; Olsson et al., 2009).

In the wider field of hydrological modelling, recent trends have been towards more process-based conceptualizations of catchment function that have been driven by model and data fusion. In particular, the increased use of water stable isotopes in undisturbed catchments has facilitated more detailed studies on understanding upscaling, flow path evaluation, mixing processes and storage dynamics across a wide range of environments (Kuppel et al., 2018; Smith et al., 2021; Tetzlaff et al., 2018). Tracer-aided models in undisturbed catchments generally conceptualize and quantify the dominant hydrological processes modulating interactions between fluxes and storage; the related flow path dynamics and associated water ages. However, urban areas are 'messy' hydrological systems with complicated juxtaposed (engineered/natural) flow path systems, additional water sources (e.g. wastewater effluent), operational water diversions (e.g. urban flood management), abstraction (e.g. crop irrigation, garden use), and continuous development of rural and urban spaces. Due to the highly complex nature of urban landscapes and the relatively limited use of water stable isotopes in urban catchments, there is a high potential for the use of water stable isotopes and tracer-aided models in urban

areas to provide richer insights into important process interactions and hydrological impacts (Ehleringer et al., 2016).

To improve understanding of process interactions and water partitioning in urban landscapes, there has been an increased use of more complex ecohydrological modelling approaches to characterize flux dynamics in urban green spaces (Gillefalk et al., 2022; Ichiba et al., 2018; Meili et al., 2020). Relatively few of these modelling approaches utilize tracers such as water stable isotopes to better constrain water flux estimations (e.g. Gillefalk et al., 2021). Rather, many of the recent modelling approaches have sought to transform the existing modelling frameworks developed for undisturbed watersheds into urban areas. With the large data requirements needed to constrain more physically based ecohydrological models in undisturbed landscapes (e.g. Kuppel et al., 2018), increased complexities within urban environments dictate that a similar approach would require an even more extensive data network (Ichiba et al., 2018). Despite the data measured from engineered structures (e.g. major abstractions, wastewater effluent, diversions), data collection is often still constrained with limited hydrometric measurements, other than climatic variables and discharge data. Using this limited data can then result in over-parameterization of more complex models (Petrucci & Bonhomme, 2014), and higher uncertainty of the role of more permeable urban green space in influencing groundwater recharge and stream flow generation (McGrane, 2016). Consequently, using isotopic data in more simple modelling frameworks, such as transit time models and mixing analysis, can provide significant insights into urban catchment functionality with fewer spatial data requirements and model parameters. These model frameworks have been successful at identifying the separation of rapid impervious-influenced flow dynamics from the more permeable areas of urban green space dominated by subsurface processes (Marx et al., 2021; Soulsby et al., 2014). Furthermore, the inclusion of evaluating water ages and transit times in such frameworks can provide the added benefit of further understanding water movement and mixing in more complex environments. However, the information content and robustness of urban catchment hydrological processes gained from models of varying complexities are not always clear. As such, there is a need for continued exploration of appropriate model complexity to integrate insights from urban water stable isotopes and take steps towards a more holistic understanding of the hydrology of urban areas.

The City of Berlin, Germany, is an extensive urban area (~900 km²) with a population of >4 million people and an annual population growth of 1% per year; it is also situated in a region with already high water stress and significant water exploitation (European Environment Agency, 2014). These coupled factors have significant implications for urban water resources given the projections of warmer and drier climatic conditions in the coming decades (Huang et al., 2013; Huang et al., 2015). Extensive surveys of surface water, groundwater, precipitation (Kuhlemann et al., 2020) and soil water (Kuhlemann et al., 2021) have characterized the stable isotopic dynamics in Berlin's hydrological systems over the past 3 years. This has resulted in considerable insights into the role of different water sources in driving stream water dynamics. In particular, intensive

water stable isotope-based investigations of hydrological processes have been undertaken within the Panke catchment within northern Berlin, which has helped quantify the relative influence of the heavily engineered systems and more natural green spaces on water movement (Marx et al., 2021).

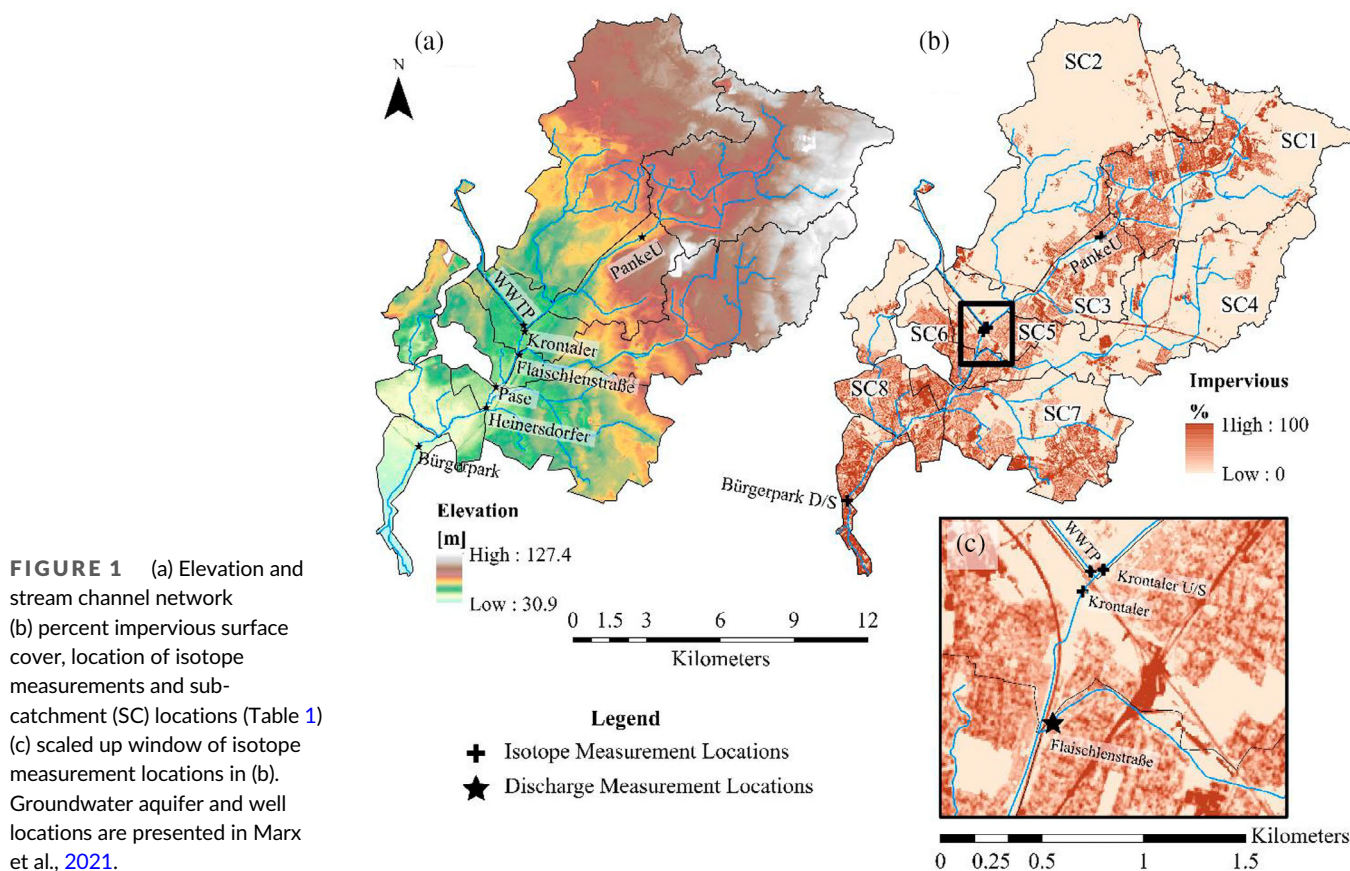
Here, we leverage that water stable isotope data with an exploration of model complexity by incorporating mixing processes with the Hydrologic Engineering Center Hydrologic Modelling Systems (HEC-HMS) model, a widely used urban runoff model. We also utilize transit time modelling to help understand the timescales of water movement within this intensively urbanized catchment. The overall aim of the article is to use isotope-aided modelling as the first step in a learning framework to guide the evolution of more realistic, integrated approaches to urban hydrological modelling, starting with reduced parameterization compared with fully distributed, urban ecohydrological models. Specifically, we aim to (1) Quantify the spatial and temporal variability of dominant streamflow components within a heavily urbanized catchment; assessing in particular, the increasing downstream influence of managed effluents and abstractions on the flow regime. (2) Evaluate hydrological model performance and process consistency through the integration of water stable isotopes and water age estimation. (3) Assess the change in isotopic dynamics and estimated stream water ages over the length of the stream due to changes in impervious areas and other anthropogenic influences (e.g. wastewater treatment plants, WWTP) on mixing. (4) Evaluate the limitations of this preliminary approach and recommend directions for

quantitative evaluation of hydrological processes with tracers within urbanizing landscapes.

2 | METHODOLOGY

2.1 | Study site background

The Panke is a mesoscale (217 km²) urban catchment; the headwaters are located in the more rural State of Brandenburg, Germany, the river then flows through the heavily urbanized landscape of Berlin before discharging into the River Spree (Figure 1). The catchment is one of the major tributaries transferring urban runoff from northern Berlin. Similar to the surrounding region, the catchment has low-lying topography, with only ~97 m of relief over the length of the catchment (~30 km) and an average catchment slope of 2.4% (Marx et al., 2021). The soils are heavily disturbed within Berlin, but primarily can be classified as freely draining sandy loams with smaller regions of loamy sand. The underlying geology was formed from deposition in the last glaciation (Frick et al., 2019), consisting of >100 m of Quaternary deposits (Limberg & Thierbach, 2002). Two aquifer systems are formed in the near-surface geological units, with a smaller, partially confined aquifer dominating groundwater-surface water exchange in the more elevated plateau in the eastern part of the catchment and the larger, unconfined Panke aquifer controlling flow through the main Panke valley (Marx et al., 2021).



Vegetation within the Panke encompasses a wide range of land uses, inclusive of conifer forests (mainly Scots Pine (*Pinus sylvestris*) (north-west, Sub-Catchment (SC) 2 in Figure 1), arable land (east, SC4 in Figure 1), and broadleaf trees and grassed areas (Table 1). Urbanized areas contribute to approximately 24% of the catchment (Marx et al., 2021). Broadleaf trees (e.g. oak (*Quercus robur*) and Birch (*Betula pendula*) and grasses dominate urban vegetation types and are found in more abundance in the southern reaches of the catchment).

The climate within the catchment is warm and temperate, with maritime influence (Köppen Index Cfb). The average annual precipitation (2011–2020) is ~590 mm, with mild annual temperatures (10.3°C) ranging from monthly averages of 1.2°C in winter to 20°C in summer (Figure 2; DWD, 2022). Large summer rainfall events are driven by high-intensity convective cells which can result in >80 mm of precipitation within a few hours (Figure 2a), while winter precipitation is more frequent, but is generally lower intensity frontal rainfall. The region is drought-sensitive, with the most recent drought (420 mm annual precipitation in 2018) causing limited groundwater recharge and vegetation stress over extensive parts of the State of Brandenburg which surrounds Berlin (Kleine et al., 2020; Smith, Tetzlaff, Kleine, et al., 2020). Total precipitation is evenly split between summer and winter rainfall contributions. Short periods of sub-freezing temperatures can occur in mid-winter (Figure 2b). Humidity undergoes seasonal cycles, with drier air during the summer (monthly average 68%) and wetter air during the winter (monthly average 88%) (Figure 2c).

2.2 | Urban catchment hydrology

Runoff generation in the Panke catchment is naturally dominated by groundwater flow in shallow sub-aquifers in the east and the primary unconfined aquifer through the main river valley flowing from north to south east (Marx et al., 2021). Flow paths through the deeper groundwater system are decadal to millennial in age, sourcing waters from outside the catchment as part of a regional aquifer which encompassed an area from the German-Polish border to Berlin (Bednorz & Brose, 2017; Massmann et al., 2007).

Anthropogenic influences on catchment characteristics, water sources and flow paths are extensive throughout the catchment due

to urbanization, land-use management and engineering structures. Throughout the catchment, urban stormwater overflows (SWOs) are estimated to contribute an annual average of 0.1 m³/s (~10% of streamflow at the catchment outlet). In the upper reaches of the catchment, SWOs are comprised of urban runoff (e.g. separate sewer storm drain), while in the lower reaches combined sewer networks incorporate higher volumes of water due to urban storm drainage and urban wastewater. The SWOs in the gauged upstream sub-catchments (SC1 and SC3, Figure 1b) are nonlinearly underlain with urban storm drains that discharge directly into the upper Panke during lower flows and overflow into the urban wastewater system during higher flows. The other northern headwater catchment (SC2, Figure 1b) has small contributions from effluent discharging from a Wastewater Treatment Plant (WWTP); with effluent feeding a wetland and forested area to artificially maintain water levels (~0.05 m³/s). Evapotranspiration from the wetland limits the influence of WWTP effluent on downstream discharge. Effluent inflow from the large Schönerlinde WWTP (serving 700 000 people) occurs in the mid-reaches of the catchment (Figure 1a, ~1m³/s baseflow), and the previous water stable isotope analysis has shown it to be the dominant water source within the main stem of the Panke (Marx et al., 2021). Increased density of urbanization occurs downstream of the effluent inflow, and is accompanied by a manually operated diversion weir (at Pase, Figure 1a) for flood control with flow directed to the neighbouring Nordgraben channel in large rainfall events. The weir operation is designed to reduce flow peaks but retain water within the canalized network downstream. In conjunction with the incised upper stream network, the canalized lower stream network is characterized among the most heavily modified riverine morphology in Berlin (Senate Department for Urban Development and the Environment, 2012).

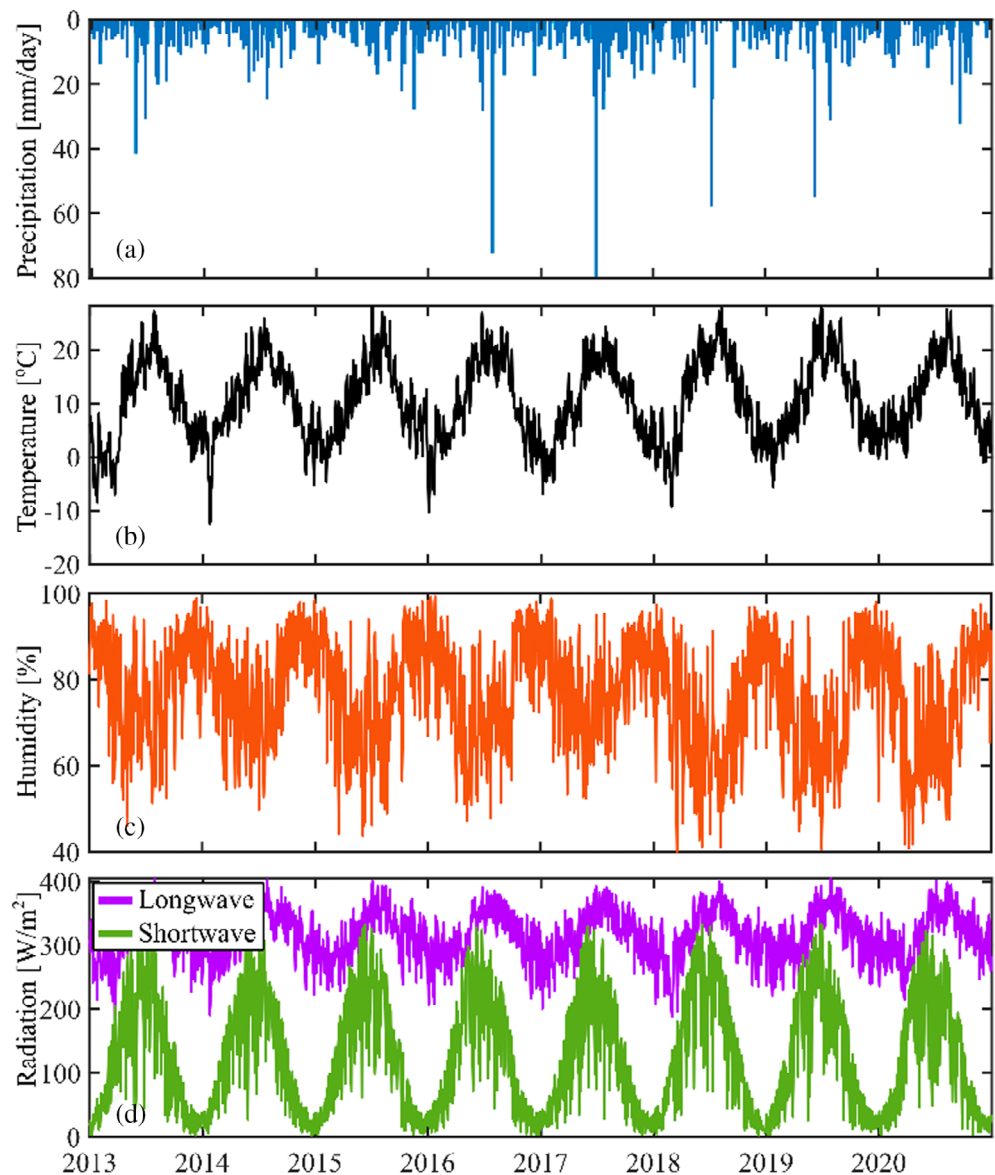
2.3 | Measured data

Climate data were available from multiple weather stations within Berlin, established and maintained by the Deutscher Wetter Dienst for precipitation, air temperature, humidity, air pressure and wind speed (DWD, 2022). Radiation data (short and longwave radiation) were available from ERA5 reanalysis datasets as hourly datasets

TABLE 1 Sub-Catchment properties of vegetation cover and total catchment area.

Sub-catchment	Impervious (%)	Broadleaf (%)	Conifer (%)	Crop (%)	Grass (%)	Area (km ²)
SC1	19.6	15.1	4.6	34.6	25.0	41.7
SC2	5.2	25.7	35.8	6.7	25.8	54.6
SC3	22.0	25.2	1.7	22.5	27.6	18.0
SC4	9.9	10.4	5.2	50.4	23.2	40.4
SC5	25.8	27.2	2.6	17.9	25.5	6.4
SC6	31.3	17.8	0.8	10.2	38.8	5.0
SC7	27.5	27.5	1.3	15.6	27.1	28.1
SC8	29.3	29.0	1.6	3.9	35.2	17.0
SC9	53.3	27.5	2.8	0.0	15.4	6.7

FIGURE 2 Climate data at Berlin Buch (52.59°N 13.45°E) climate station within the Panke for (a) precipitation (b) air temperature and (c) humidity (DWD, 2022). (d) Radiation data from ERA5 Reanalysis products within the catchment (Hersbach et al., 2019).



(Hersbach et al., 2019; Figure 2d) Senate Department for the Environment, Transport and Climate Protection (SenUVK, 2021). Four of the measurement locations are along the main stem of the Panke, with an additional measurement of tributary water level at Fleischlenstraße which is runoff from an area dominated by arable agriculture (Figure 1a,b). Wastewater from Schönerlinde WWTP has partially discharged into the Panke since 2015 (SenUVK, 2021), and additional measurements of diverted water outflow (Pase) into the Nordgraben were available from 2011. Water level was translated to discharge using established rating curve (developed by the Senate Department). Rating curves were updated as necessary through periodic evaluation against measured discharge. Infrequent high flow gauging to establish the upper range of the rating curve and potential sedimentation and seasonal channel vegetation growth can create some uncertainty in the rating curves.

Precipitation water samples for isotope analysis were taken using an autosampler at the Urban Ecohydrological Observatory at Steglitz

(10 km south of Panke) (Kuhlemann et al., 2021). Samples have been collected since the beginning of 2019, with additional grab samples at Berlin Buch climate station within the Panke taken during 2020, which showed good comparability with Steglitz (Marx et al., 2021). A layer of paraffin (3 mm) was added to all sample containers to prevent evaporation. Stream water samples were taken through grab sampling throughout the Panke from October 2019 to December 2020 (locations on Figure 1b). Samples were taken monthly until April 2020, and from April 2020 to December 2020 biweekly sampling increased temporal sample resolution. Stream sampling included three upstream locations (PankeU, Krontaler U/S and Krontaler, Figure 1b) with further sampling of the WWTP effluent. Stream water downstream of Bürgerpark was sampled daily (Figure 1b). Sampling of the local aquifer system was conducted monthly (Marx et al., 2021).

Water samples were decanted and filtered (2 μm cellulose acetate) and refrigerated until water stable isotope measurement. Cavity Ring-Down Spectroscopy was conducted using a L2130-I Isotopic

Water Analyser (Picarro, Inc. Santa Clara, USA, 2020) for deuterium ($\delta^2\text{H}$) and oxygen-18 ($\delta^{18}\text{O}$). Analytical precision was $\pm 0.1\%$ and $\pm 0.025\%$ for $\delta^2\text{H}$ and $\delta^{18}\text{O}$, respectively. Analysis of water samples was conducted with periodic measurement of known isotopic standards to verify measurement accuracy. Further details on isotopic standardization are presented in Marx et al. (2021).

2.4 | Hydrological modelling system (HEC-HMS)

The Hydrologic Engineering Center Hydrologic Modelling System model was developed by the US Army Corps of Engineering for dendric watersheds and incorporates numerous model structural components to address both short-term (event-based) and long-term (multi-year) hydrological analysis (Feldman, 2000). Model structure options are available for evapotranspiration, canopy and surface storages, infiltration, surface runoff transform method, baseflow, and flood routing, with parameterizations of processes defined for each sub-catchment. Details of the utilized model structure components are presented below, with more detailed descriptions of other model structure options provided in Feldman (2000) and Scharffenberg and Fleming (2008).

Spatial distribution of water storage and fluxes (Figure 3) is conducted at a sub-catchment scale. Outflow from each sub-catchment is collected by the stream network and routed downstream. The effects of vegetation on sub-catchment water availability are considered

using a simple canopy bucket storage approach, which considers maximum canopy storage, canopy crop coefficient and root-water usage method. Incoming precipitation is intercepted by canopy storage until canopy storage is filled (Figure 3). Excess precipitation is transmitted to the land surface, while canopy storage is emptied by evaporation prescribed by the potential evapotranspiration rate. Precipitation reaches the land surface which is categorized as either directly connected impervious surfaces or pervious surfaces. Precipitation on impervious surfaces is translated to direct flow to the channel (Q_d), while precipitation on pervious surfaces (surface storage, Figure 3) are subject to the model structure for hydrological partitioning and loss estimations (Figure 3). Infiltration from pervious surfaces is assumed to an average representation of infiltration in all previous areas in the sub-catchment.

To provide simulations of both storage dynamics and associated fluxes for tracer mixing, the hydrological loss is estimated using the soil moisture accounting loss method (Bennett & Peters, 2000) (Figure 3). Surface water on pervious surfaces is available for infiltration to the soil storage at the beginning of each time-step, with potential infiltration rates ($i_{\text{pot}}(t)$) and capacity determined by the maximum infiltration rate (i_{max}), and the current and maximum soil storage ($S(t)$ and S_{max}):

$$i_{\text{pot}}(t) = i_{\text{max}} \left(1 - \frac{S(t)}{S_{\text{max}}} \right). \quad (1)$$

Water that does not infiltrate remains in the surface storage until the water is either evaporated or infiltrates in the subsequent time-steps. Surface water exceeding the maximum depression storage is translated to the channel as direct flow. Soil storage is partitioned into upper zone storage and tension zone storage, where all soil storage only loses water to evapotranspiration, and only the upper zone storage can percolate to deeper water storages. Flow into and out of deeper storages (two storages) is defined through the percolation rates:

$$P_{\text{pot}}(i,t) = P_{\text{max}}(i) \left(\frac{S(i,t)}{S_{\text{max}}(i)} \right) \left(1 - \frac{S(i+1,t)}{S_{\text{max}}(i+1)} \right), \quad (2)$$

where $P_{\text{pot}}(i,t)$ is the potential percolation from storage in layer i , and is dependent on the maximum possible percolation rate ($P_{\text{max}}(i)$) and the ratio of current soil storage volumes ($S(i,t)$) to maximum storage volumes (S_{max}) of layer i and layer $i+1$. The actual percolation ($P_{\text{act}}(i,t)$) is the minimum of the potential percolation and the available water for percolation. The lateral flow (Q_g) out of the deeper storages (not soil storage) is defined using the vertical water balance and a routing storage parameter (GW_R):

$$Q_g(i,t+1) = \frac{P_{\text{act}}(i-1,t) + S(i,t) - P_{\text{pot}}(i,t) - 0.5Q_g(i,t) * t}{GW_R + 0.5 * t} \quad (3)$$

with the total volume (V) of water released from storage:

$$V(i,t) = 0.5(GW_Q(i,t+1) + GW_Q(i,t)) * t. \quad (4)$$

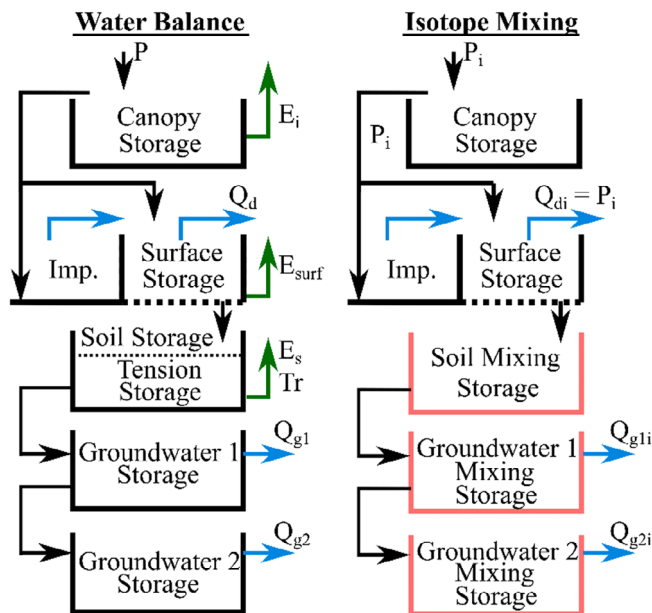


FIGURE 3 Schematic of the sub-catchment model structure. Schematic of the isotope mixing module. Storage mixing for isotopes adds passive storage to the water balance output from HEC-HMS. Surface storage is representative of pervious soil regions. P is precipitation, Imp is impervious, E_i is interception evaporation, Q_d is direct flow, E_{surf} is evaporation from surface storage, E_s is soil evaporation, Tr is transpiration, Q_{g1} is lateral flow from groundwater storage 1, and Q_{g2} is lateral flow from groundwater storage 2.

The sub-catchment hydrograph transformation is estimated using the Snyder unit hydrograph method. This uses unit hydrographs to translate catchment runoff to sub-catchment hydrograph peak flows (Feldman, 2000). River flood routing in channelized reaches is estimated using the Muskingum–Cunge approach (Cunge, 1969), using channel length, slope, Manning's n values, and channel shape to route water. Channel shape was assumed to be rectangular to simplify calculations, and automatic estimation of space and time-step for routing was used to ensure numerical stability.

The Penman–Monteith method (Monteith, 1965) is used to estimate potential evapotranspiration using a combination of energy balance and mass transfer approaches (Allen et al., 1998). Potential evapotranspiration is estimated using short- and long-wave radiation, wind speed, air temperature, air and vapour pressure in conjunction with a reference albedo and crop coefficient to account for differences in vegetation and aerodynamic resistance.

2.5 | Water stable isotope mixing and flow components module

Mixing of water stable isotopes ($\delta^2\text{H}$ and $\delta^{18}\text{O}$) and water ages was conducted using the estimated fluxes and storages from calibrated results of the HEC-HMS model. Thus, the isotopes were not used as a calibration constraint for flux quantification, but rather as an independent check on the simulations. To incorporate the additional effects of passive storage on damping the isotopic dynamics (e.g. Birkel et al., 2011), an additional storage parameter for the soil, upper and lower groundwater storages was included in addition to the dynamic storage simulated by water balance variations. Mixing within each storage (dynamic + passive) is conducted using amount-weighted, complete and uniform mixing assumptions for each time-step as with other isotopic modelling approaches (Ala-Aho et al., 2017; Kuppel et al., 2018). At the end of each time-step, one time-step is added to each average water age in storage to account for the ageing of water. As fractionation in the stream was previously identified as negligible except for the WWTP effluent component (Marx et al., 2021), fractionation effects from evaporation were also assumed to be negligible and were not considered within the isotope mixing module. WWTP effluent isotopic compositions were added as measured external source water to the catchment.

2.6 | Parameterization, calibration and uncertainty analysis

The HEC-HMS model was set up to best utilize the available discharge and stream isotope datasets by setting sub-catchment drainage areas to each measurement location. Further consideration was made for differences in regional landcover characteristics (Table 1). The model was set to run on 12-h time-steps to balance representation of rapid event-based urban runoff effects as well as groundwater-generated

baseflow component. Model testing was used to identify sensitive parameters to be used in calibration (Table S1), which primarily revealed the soil water loss parameters as the most sensitive parameters for calibration. Insensitive parameters were held constant at default values. WWTP effluent was added as an additional source of water using measured inflow time-series above Krontaler (Figure 1a), and a diversion element was included with measured diverted discharge to incorporate the manual operation of the weir at Pase (Figure 1a). The model was set up to run from January 2013 to December 2020, using the first 2 years as model spin-up as WWTP effluent was not measured until 2015.

Input forcing data (Section 3.1) included data from the surrounding weather stations (DWD, 2022) and re-analysis datasets for short- and long-wave radiation (Hersbach et al., 2019). Measured DWD climate data (DWD, 2022), in particular the timing and quantity of precipitation events, were compared to evaluate the spatial heterogeneity of precipitation and incorporate this in the modelling approaches. Precipitation amount and timing notably differed from the northern to the central sub-catchments (i.e. precipitation north of SC2 to Berlin Buch station in SC3), with the northern stations receiving less rainfall than the southern stations. Therefore, the two northern catchments (SC1 and SC2) utilized a distance weighted precipitation input.

To enable the model spin-up of the isotope mixing module, a stochastic model was created for isotopic precipitation inputs from 2013 to the beginning of measurement in 2019. The stochastic model utilized precipitation amount, temperature, humidity, wind speed, and a randomization factor fit against measured data (2019–2020, $R^2 = 0.89$). Used for spin-up purposes only, this generated long-term dataset is presented in Figure S1. The isotopic WWTP effluent was gap-filled to produce a continuous input time series for downstream locations. On comparative sample days (weekly sampling) over a two-year period, variability in in WWTP effluent isotopic signatures was much lower than stream water (standard deviation $\sim 1.5\%$ v. 4.7% for $\delta^2\text{H}$ for WWTP and streamwater, respectively). Gap filling was conducted using a simple approach with the mean and a randomization term defined using the percentiles of measured data, in a method similar to bootstrapping. As much of the observed variability was due to larger convective events, and WWTP discharge variability was low, average variability (daily) is likely lower than observed variability.

Calibration of HEC-HMS was conducted using the optimization toolbox with the Simplex Search Algorithm (Lagarias et al., 1998). Maximum iterations were set to 1000 with an objective tolerance (rate of change of Nash–Sutcliffe efficiency, NSE; Nash & Sutcliffe 1970) set to $1 \text{ E-}4$. Calibration search criteria (iterations and tolerance) were evaluated throughout the calibration to ensure that the criteria did not influence search objectives. The convergence of the model parameters to the global maximum through the optimization algorithm was tested by changing initial parameters.

For consistency in calibration approaches, the isotope module used the Simplex Search Algorithm set-up in Matlab[®]. We utilized the *fminsearchbnd* package (D'Errico, 2022) to define the upper and lower

parameter bounds, and calibrated using the NSE (Nash & Sutcliffe, 1970), Kling-Gupta (KGE) (Gupta et al., 2009), and mean absolute error (MAE). The NSE and KGE were multiplied by -1 to provide a minimum search value. Similar to the HEC-HMS calibration, changes in initial values were tested to ensure a global maximum was reached.

Model uncertainty was evaluated for all model outputs using the Generalized Likelihood Uncertainty Estimation (GLUE) methodology (Beven & Binley, 1992). The CURE toolbox (Page et al., 2022) was used to model uncertainty bounds, defined as the output 95th percentiles.

2.7 | Transit time estimations

Mean transit times (MTTs) of streamflow at various locations throughout the catchment were estimated independently using the measured $\delta^2\text{H}$ in precipitation and in streamflow. We used a two-parallel linear reservoir (TPLR) transit time model which has previously been shown to be effective in peri-urban environments in accounting for differences in urban and nonurban areas and contrasted results to the more commonly used gamma distribution transit time model which has been shown to be applicable to a wide range of catchments (Godsey et al., 2010). Input precipitation $\delta^2\text{H}$ was weighted by amounts in the convolution equation:

$$C(t) = \frac{\int_0^t C_{in}(t-\tau)P_{in}(t-\tau)g(\tau)d\tau}{\int_0^t g(\tau)P_{in}(t-\tau)d\tau}, \quad (5)$$

where τ is the transit time, $C(t)$ is the isotopic composition in streamflow, $C_{in}(t-\tau)$ is the input isotopic composition at time $t-\tau$, $P_{in}(t-\tau)$ is the precipitation at time $t-\tau$ and $g(\tau)$ is the transit time distribution given for TPLR as follows:

$$g(\tau) = \frac{\phi}{\tau_f} \exp\left(-\frac{\tau}{\tau_f}\right) - \frac{(1-\phi)}{\tau_s} \exp\left(-\frac{\tau}{\tau_s}\right). \quad (6)$$

The transit time distribution has three parameters, ϕ is the fraction of fast water flow (0–1, e.g., urban storm flow), τ_f and τ_s are the mean residence times of the fast and slow flow reservoirs. Transit times estimated downstream of WWTP effluent utilized HEC-HMS simulations to define the contribution of WWTP water in stream:

$$C_{out}(t) = C(t) \left(1 - \frac{Q_{WWTP}(t)}{Q(t)}\right) + C_{WWTP}(t) \left(\frac{Q_{WWTP}(t)}{Q(t)}\right), \quad (7)$$

where $Q_{WWTP}(t)$ is the total flow from WWTP in the stream at time t and $Q(t)$ is the total flow in the stream at time t . The transit time model was calibrated using the Simplex Search Algorithm in Matlab[®] (D'Errico, 2022) using NSE, KGE and MAE.

3 | RESULTS

3.1 | Discharge and source water contribution

The HEC-HMS model reproduced seasonal discharge dynamics and general responses throughout the catchment reasonably well (Figure 4 and Table 2); however, the heavier emphasis of the NSE on peak flows revealed a limitation of the model and especially the input data to capture all precipitation events; especially summer convective cells. These high peaks primarily occurred in the headwater catchments (discharge at PankeU, Figure 4a), where the magnitude of most peak events was under-estimated (e.g. summer convection events in 2017–2019). In particular, the measured peak flow event in mid-2017 experienced a multi-day lag which was not evident in the precipitation, and the extent of the lag was not observed for other events or in the other sub-catchments. Additionally, measured discharge events occurred without measured precipitation (e.g. 2019 peak, Figure 4a), revealing the influence of precipitation heterogeneity. Discharge in the mid-eastern sub-catchments (discharge at Flaischlenstraße, Figure 4c) had only minor deviations with the exception of the 2017–2018 winter; however, the underestimation did not propagate downstream (discharge at Heinersdorfer, Figure 4d). Discharge at Krontaler (Figure 4b) had a slight over-estimation in 2018 and 2019, but showed a good representation of discharge dynamics downstream of the WWTP inflows (Table 1, discharge KGE). Discharge estimations improved further downstream of the diversion (Table 1), with more minor event-based deviations from measurements. The largest downstream deviation occurred at Bürgerpark at the beginning of 2020 where simulated discharge notably exceeded measured discharge (Figure 4 e). This deviation was not evident in the simulations immediately upstream at Heinersdorfer (Figure 4 d).

Simulations from tributary and headwater catchments (Figure 4 f, h) were dominated by deeper groundwater contributions, with shallower sub-surface sources of interflow providing an increased contribution to streamflow during winter months. Direct flow peaks from surface runoff occur in both the summer and winter months, driven by larger precipitation events. Discharge locations downstream were heavily influenced by the WWTP effluent contributions (Figure 4 g, i, j), which dampened discharge dynamics and produced a much higher baseflow component (Figure 4 b, d, e). The WWTP contribution to streamflow was greatest during the summer months when upstream discharge contributions were lower (e.g. Figure 4 a). The simulated total contribution of WWTP effluent was similar to measured discharge-based estimations (dashed line Figure 4 g), with a modelled under-estimate when discharge was over-estimated (Figure 4 b). Through most of the mainstream channels, WWTP effluent contribution increased during the 2018 summer drought, exaggerating the influence of WWTP effluent on baseflow conditions. WWTP contributions were damped further downstream (Figure 4 i, j) through further tributary contributions. These contributions were exaggerated by the diversion of water at Pase which removed $\sim 0.85 \text{ m}^3/\text{s}$ ($\sim 45\%$ of discharge) and greatly impacted the total contribution of WWTP water.

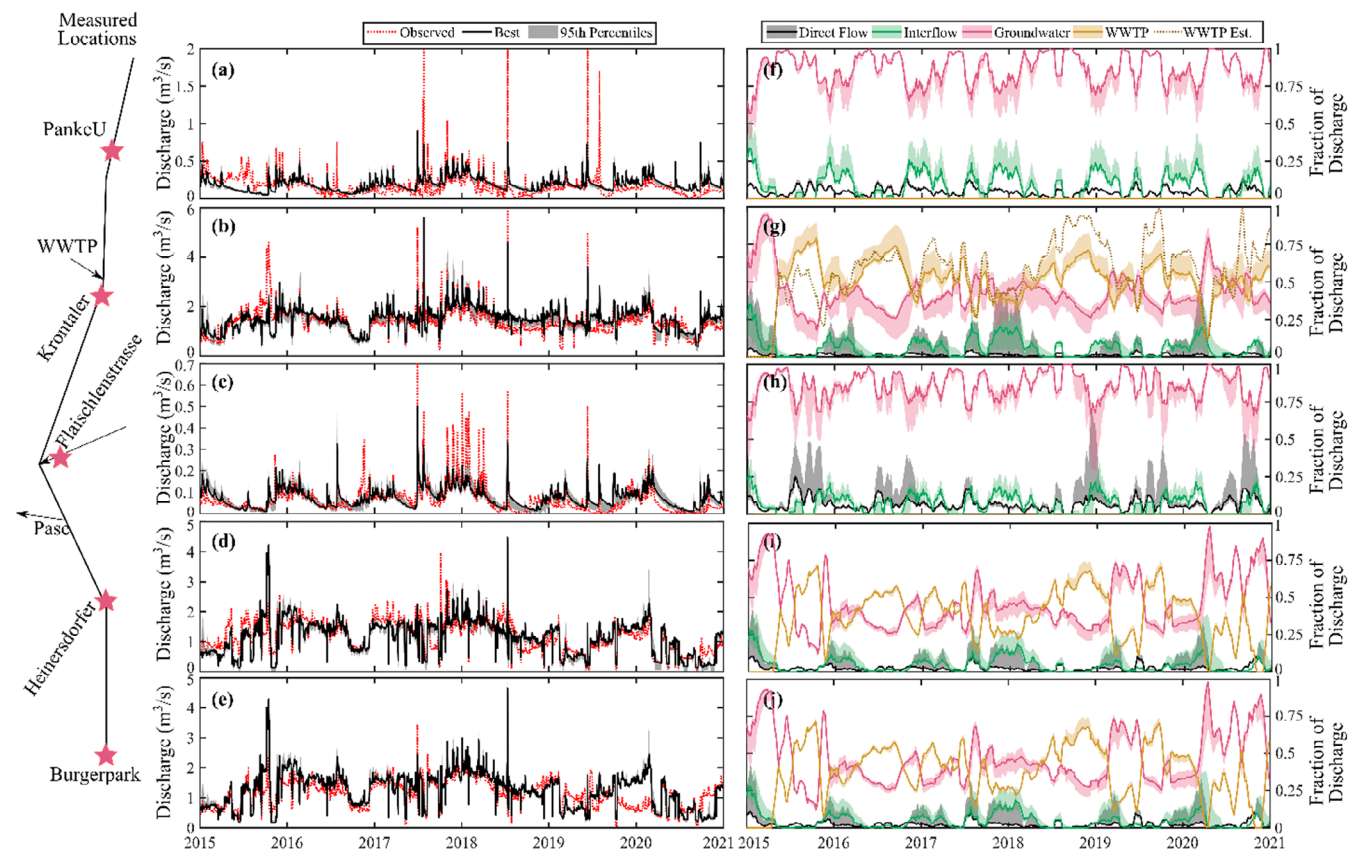


FIGURE 4 Simulated discharge at major sampling sites, shown in relation to the simple schematic on the left of the figure at (a) PankeU, (b) Krontaler, (c) Flaischlenstrasse, (d) Heinersdorfer and (e) Burgerpark. The contribution of flow for each discharge site from direct flow, interflow, groundwater, and added wastewater are in subplots *f–j* respectively. The dashed line in subplot *g* represents the estimated total contribution of WWTP effluent using measured discharge only. For visual aid, the contributions are displayed as moving monthly averages.

TABLE 2 Efficiency criteria from HEC-HMS (discharge), isotope mixing module (IM) and transit time calibration. Values presented are the best-obtained efficiency criteria. Discharge efficiency is shown with NSE and KGE in parentheses.

Location	Discharge	Isotope mixing $\delta^2\text{H}$ (KGE)	TPLR TTD $\delta^2\text{H}$ (KGE)	Gamma TTD $\delta^2\text{H}$ (KGE)
PankeU	0.14(0.26)	0.59	0.65	0.71
Krontaler U/S	N/A	0.55	0.46	0.41
Krontaler	0.45(0.73)	0.86	0.72	0.68
Flaischlenstraße	0.40(0.48)	N/A	N/A	N/A
Heinersdorfer	0.51(0.69)	N/A	N/A	N/A
Burgerpark	0.50(0.74)	0.40	0.48	0.47

3.2 | Stream water stable isotopes and mean water ages

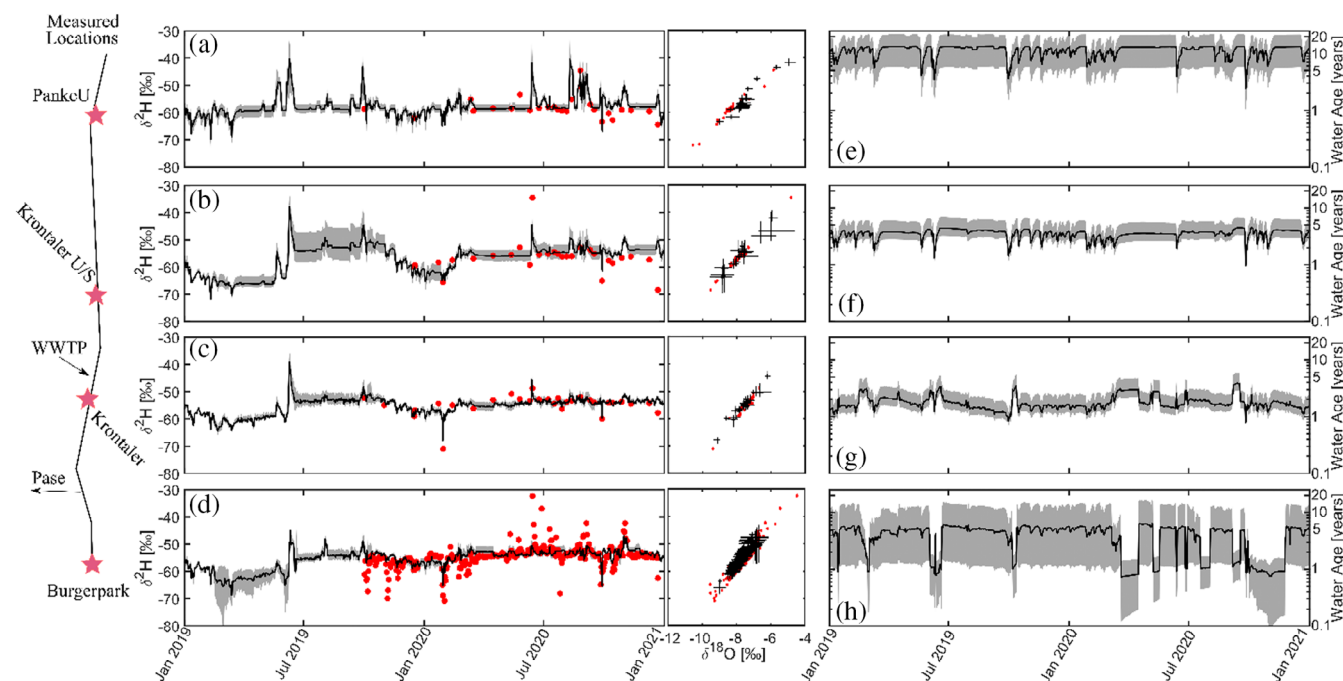
The isotope mixing module with an additional passive storage component (Table 3) produced satisfactory simulations of water stable isotopes in stream water throughout the catchment (Figure 5 and Table 1). Although the presented results focus on $\delta^2\text{H}$, simulations for $\delta^{18}\text{O}$ were of a similar quality (see insets in Figure 5). Larger events in the upstream sites were well captured, though there was a slight over-estimation of baseflow isotopic signals towards the end of the simulation (Figure 5a,b). The WWTP effluent immediately

downstream damped the isotopic dynamics and further reduced the uncertainty (Figure 5c) due to the large contribution of inflows (Figure 4g). Daily sampling at the outlet revealed higher isotopic variability than was evident in the less frequently sampled upstream sites. The mixing module was able to capture the general dynamics (Table 1) in addition to some of the larger precipitation events; however, some summer convective events (e.g. June and July 2020) were not captured by the model due to the high groundwater contribution that was simulated (Figure 4i,j).

Estimated water ages (from isotope mixing) in the stream decreased from the tributaries to the outlet (Figure 5e). In the

TABLE 3 Mean and standard deviation of passive storage (mm) additions to shallow soil, groundwater, and deep groundwater storage used for water stable isotope mixing at different locations within the catchment.

	Shallow soil storage	Shallow groundwater storage	Deeper groundwater storage
Upstream (SC1)	7.77 ± 3.9	96.4 ± 23.73	1929.52 ± 236.5
Mid-Reach (SC2-SC5)	0.21 ± 0.73	0.12 ± 0.47	22.09 ± 17.74
Downstream (All remaining sub-catchments)	60.79 ± 12.98	97.52 ± 54.07	7.46 ± 7.86

**FIGURE 5** Simulated (mean and 95 percentiles) and measured (red circles) stream deuterium from the mixing module in (a) PankeU, (b) Krontaler U/S, (c) Krontaler and (d) Burgerpark. Measured and simulated isotopes in $\delta^2\text{H}-\delta^{18}\text{O}$ space are shown for each time series. Estimated mean water ages for each site are shown in subplots e–h, respectively. Note that there is a compression of the spatial scale on the schematic for the downstream reaches (Krontaler to Burgerpark).

upstream catchment, the mean age of water was ~ 11.6 years with younger water influences during rainfall events driving the simulated age of storm events to ~ 2.2 years; however, the water age estimates had large uncertainty. Water ages reduced further downstream (before the WWTP inflow), with a mean water age of ~ 3.6 years and event-based depressions to ~ 0.6 years (Figure 5f). The much younger water ages additionally reduced the water age uncertainty (Figure 5f). The contribution of WWTP effluent (inflow age of 0 days) further reduced estimated average water ages (~ 2.2 years), but increased event variability due to WWTP effluent controls (Figure 5g). While there was increased impervious area percentages towards the south of the catchment, higher simulated groundwater contribution (Figure 4j) slightly increased the simulated water ages towards the outlet of the catchment (Figure 5h) with a mean age of ~ 4.5 years (event-based variability ~ 2.9 years). Increased uncertainty at the outlet was the result of divergence of water age estimates from different efficiency criteria (Table 4). The divergence of water age estimates was only present at the outlet due to the increased data availability (daily data) which further revealed more variability

than the biweekly data. Larger, nonlinear variability of water age in the southern reaches of the catchment reflected the diversion of high flows out of the catchment at Pase with smaller upstream volume to dampen the incoming younger water from the southern sub-catchments.

3.3 | Transit time distributions and water ages

Similar to the isotope mixing module, the transit time modelling approach yielded satisfactory results for the water stable isotope time-series at the stream sites throughout the catchment (Figure 6 and Table 1). Like the mixing module, simulations late in the period (end of 2020) for $\delta^2\text{H}$ stream values were overestimated, with a larger deviation in the transit time model (Figure 6a,b). Additionally, the influence of large precipitation events (e.g. June 2020) were not apparent within the transit time models (Figure 6b). Similar to the isotope mixing module, isotopic dynamics and uncertainties were reduced downstream of the WWTP inflow (Figure 6c). Water stable

TABLE 4 Mean water ages (\pm temporal variability, in years) of streamwater at different locations in the catchment for each model and efficiency criteria. Note that the mean water ages include all 'best' model parameter sites.

		Average water age from each efficiency criteria		
		KGE	NSE	MAE
Isotope Mixing Module	PankeU	18.9 \pm 3.7	8.9 \pm 1.6	7.0 \pm 1.4
	Krontaler U/S	5.2 \pm 1.0	2.8 \pm 0.5	2.7 \pm 0.4
	Krontaler	3.3 \pm 1.7	1.8 \pm 0.9	1.7 \pm 0.9
	Burgerpark	10.9 \pm 7.9	1.3 \pm 0.4	1.3 \pm 0.4
Two parallel linear reservoir TTD	PankeU	1.1 \pm 0.3	2.1 \pm 0.5	1.8 \pm 0.3
	Krontaler U/S	1.1 \pm 0.4	1.6 \pm 0.3	1.5 \pm 0.3
	Krontaler	0.2 \pm 0.2	0.5 \pm 0.3	0.4 \pm 0.2
	Burgerpark	0.3 \pm 0.2	0.5 \pm 0.2	0.6 \pm 0.2
Gamma TTD	PankeU	0.4 \pm 0.1	2.0 \pm 0.3	2.2 \pm 0.3
	Krontaler U/S	0.4 \pm 0.1	1.3 \pm 0.1	1.1 \pm 0.1
	Krontaler	0.1 \pm 0.1	0.4 \pm 0.2	0.3 \pm 0.2
	Burgerpark	0.2 \pm 0.1	0.6 \pm 0.2	0.6 \pm 0.2

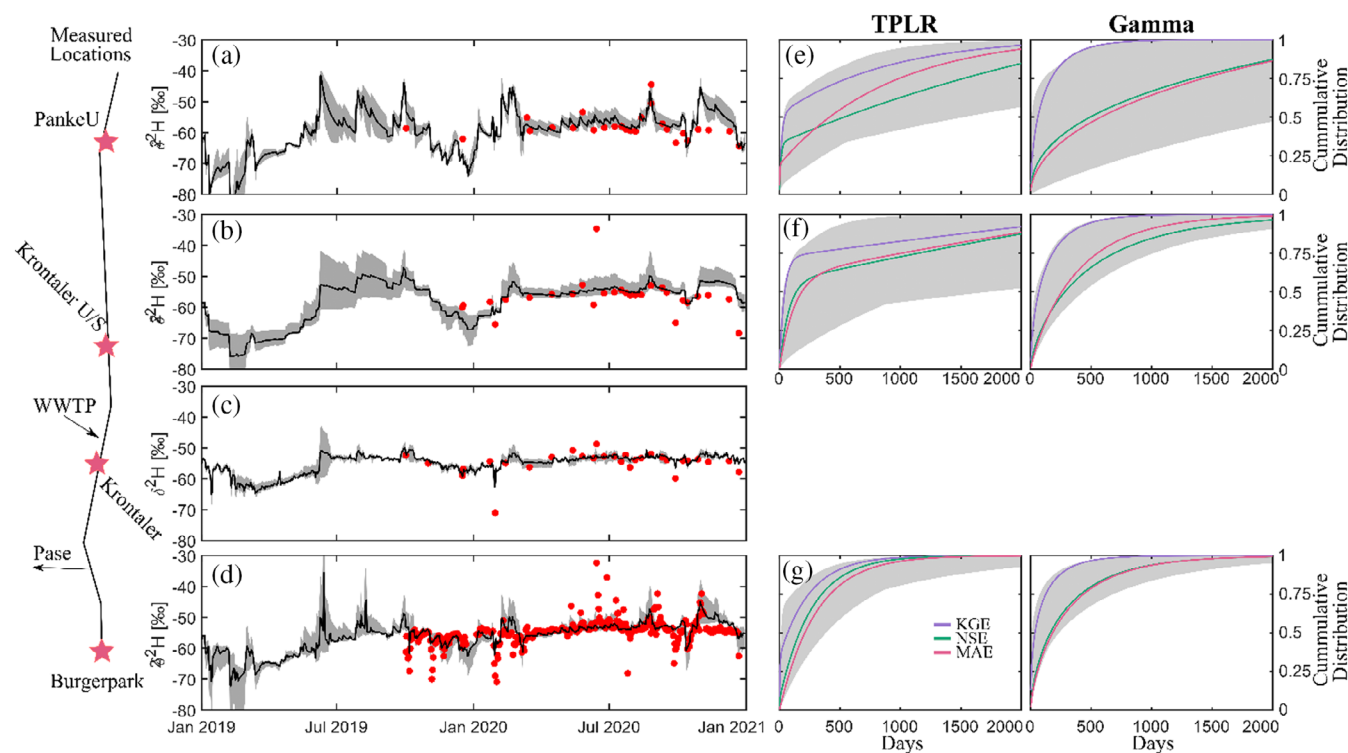


FIGURE 6 Simulated TPLR stream deuterium and cumulative transit time distributions of two parallel linear reservoir (TPLR) and Gamma functions for (a and e) PankeU, (b and f) Krontaler U/S, (c) Krontaler, and (d and g) Burgerpark. The range in median water age is shown for each site. Krontaler isotopes are a mixture of Krontaler U/S and WWTP inflow (no calibrated transit time distribution) and that there is a compression of the spatial scale on the schematic for the downstream reaches (Krontaler to Burgerpark).

isotope dynamics were increased towards the outlet; however, similar to the mixing module, the transit time models were unable to capture the larger day-to-day variability from convective precipitation at the outlet (e.g. June and July 2020).

Water ages generally decreased from upstream to downstream with the exception of the TPLR transit time model at Krontaler U/S

(Table 4). Estimated transit times in the upstream sites (Figure 6e,f) showed wide uncertainty bounds for both transit time models despite relatively narrow isotopic bounds (Figure 6). The TPLR TTD model showed an increasing proportion of water from the fast-flowing reservoir (higher slope for shorter transit times) with increased distance downstream, mirroring the increase in impervious surfaces

downstream. Uncertainty in the transit time and water age estimates decreased towards the outlet of the catchment (Figure 6g).

Average water ages at different locations in the catchment varied depending on the model used (isotope mixing module or TTD) and on the efficiency criteria used for optimization (Table 4). The TTD models consistently revealed younger water ages than were estimated from the isotope mixing module (Table 4) and were most noticeable in the headwater catchment (PankeU, Table 4). The difference between the isotope mixing module and TTD models were reduced further downstream where younger water and WWTP effluent dominated streamflow. The use of different efficiency criteria revealed their importance for the evaluation of water ages for both the mixing module and TTD models. Using the NSE and MAE as optimization efficiency produced relatively consistent water ages and isotopic simulations (Table 4), while KGE produced notably different water age estimates without significant changes to the isotopic simulations (Figures 5 and 6 and Table 4). In the isotopic mixing module, the KGE optimization greatly increased water age estimations, while decreasing water age estimations in TTD estimations.

4 | DISCUSSION

4.1 | Evaluating urban hydrological processes

Through the application of relatively simple model frameworks as learning tools, we could use isotope data and the concept of water age to gain insights into spatiotemporal patterns of hydrological function within a heavily modified urbanizing landscape. This helped to constrain the identification of dominant catchment-scale flow paths and water sources, as well as to identify how key processes changed through wet, and in particular, dry years (e.g. 2018 and 2019) which will likely occur through much of Europe more frequently under climatic change (Cammaleri et al., 2020; Gudmundsson & Seneviratne, 2016).

By utilizing a simple semi-distributed model framework, we gained further insights into the likely importance of groundwater and shallow subsurface contributions to streamflow at multiple locations within the catchment. In the northern, more rural regions of the catchment in Brandenburg, the simulated high proportion of streamwater contribution from groundwater (Figure 4f) was broadly consistent with previous tracer-based mixing models of source apportionment in the catchment (Marx et al., 2021). This is more generally similar to the dominant runoff processes identified for other rural catchments surrounding Berlin (Smith et al., 2021; Smith, Tetzlaff, Gelbrecht, et al., 2020; Wu et al., 2022). However, unlike such rural groundwater-dominated catchments where flow variations are mostly seasonal and large storm-event driven flow peaks are rare, both small and large events are evident in the Panke. Unsurprisingly, this reflects direct runoff contributions from impervious surfaces translating rapidly to the stream, as has been shown in other peri-urban catchments (Soulsby et al., 2015), though their overall contributions to annual stream flow are relatively small. However, the simple model structure

and calibration was unable to capture some of the larger events (Figure 4). Missed peak events in modelling the upper catchment could be due to multiple factors including the complex distribution of SWO thresholds that were spatially variable within the catchment or high heterogeneity of urban precipitation inputs (Liu & Niyogi, 2019; Lorenz et al., 2019). Given the limited number of these events, and their occurrence during summer, peak flows also may be uncertain due to limited measurements to characterize peak flow rating curves (Sikorska et al., 2013; Westerberg & McMillan, 2015) and/or the impact of vegetation in the channel overbank increasing rating curve uncertainty during peak flow events when over bank flow occurs (Perret et al., 2020). Furthermore, while heterogeneity in precipitation sources was incorporated within the modelling framework, known uncertainties particularly of convective precipitation heterogeneities within urban landscapes likely affect event-based discharge simulations during summer (Meierdiercks et al., 2010; Singh et al., 2020). The effects of urbanization on rainfall spatial patterns and quantities may also be affected by the degree of urbanization, where spatial differences have been shown between urban core areas and suburbs (Yang et al., 2021). In catchments like the Panke, covering spatial heterogeneity from the urban core to suburbs and more naturalized areas, high-spatial resolution precipitation distribution networks may be needed to reduce discharge modelling uncertainties of summer peak flows (via missed events).

Spatially, the model highlighted the importance of soil storage within peri-urban catchments, where maximum soil storage changed from upstream to downstream at rates inversely proportional to the increase in impervious surfaces (Table S1). These soil storage dynamics govern percolation (Equation 2), whereby the smaller maximum storages of groundwater in the model domain facilitate more rapid water movement consistent with a shallow groundwater system. The importance of such shallow groundwater systems for the rapid development of storm runoff is consistent with other urban studies (e.g. Berthier et al., 2004).

The actual evapotranspiration estimated within the model (Table S2) was within the range of estimates for previous study sites in Berlin (Gillefalk et al., 2021, 2022; Kuhlemann et al., 2021); however, the water loss estimates were at the low-end of feasible ranges. The estimates may be lower than expected due to multiple factors, including the lower influence of green space sensitivity due to the calibration bias to blue water fluxes at the sub-catchment scale, and the differences in model structure on estimation (e.g. single v. multi-layer root-water uptake and Penman v. energy balance approach) (e.g. Duarte Rocha et al., 2022). The inclusion of total ET (and dynamics) within the calibration process has been shown to improve the overall performance of modelled ET volume in other studies (e.g. Kuppel et al., 2020); however, this will likely result in a degradation of discharge performance (e.g. summer peak flows) and due to the complexity of the hydrology (and limited spatial ET data availability), consideration should be given to evaluating the feasibility of parameter ranges controlling ET.

Lastly, the model revealed the sensitivity of the estimated flow contributions to process uncertainties and temporal variability. This

was most apparent immediately downstream of the WWTP effluent inflow, where the model under-estimated the significance of the WWTP effluent as a percent of contribution within the stream due to the over-estimation of streamflow upstream of the effluent (2018–2020, Figure 4a). With the over-estimation of flows late in the simulation period likely driven by an underestimation of evapotranspiration during drier periods, the significance of more constrained evapotranspiration estimations is highlighted. Downstream, the proportion of summer streamflow derived from WWTP effluent (max ~73%) was similar to previous end-member mixing estimates (80%) (Marx et al., 2021), and underlines the higher importance of WWTP effluent for maintaining summer baseflows. However, model results revealed more temporal variability than end-member mixing (Figure 4), suggesting increased groundwater and subsurface flow contributions during winter recharge events. Modelled estimates and dynamics were relatively consistent with the long-term separation of downstream discharge into upstream and WWTP effluent (Figure 4g), and may suggest more adequate capture of event-based variability that was not possible previously with 3-month isotope mixing windows (Inamdar et al., 2013; Marx et al., 2021).

4.2 | Effect of urbanization on catchment water stable isotopes and water ages

Using the fluxes and storage dynamics from the semi-distributed model with uniform and complete isotopic mixing assumptions in individual model stores, stream water isotopes were reasonably reproduced and were relatively well-constrained around the measurements. As with other lumped storage models incorporated with water stable isotopes (Birkel et al., 2011), the addition of passive storages (i.e. for relatively slow moving water) was necessary to account for isotopic damping (Table 3). The passive storage revealed the dominant influence of groundwater mixing within the upper catchment, further to additional storage and mixing than in the more urbanized downstream catchments. Despite the under-estimated WWTP effluent contribution immediately downstream (Figure 4g), resulting from an over-estimated groundwater contribution (with similar isotopic signature, Marx et al., 2021), both $\delta^2\text{H}$ and $\delta^{18}\text{O}$ were well simulated.

As with the isotope mixing module, both functional forms of transit time models (TPLR and gamma) were able to reproduce stream water isotopes, though the mixing module generally produced better isotopic simulations and the TPLR performed better than the gamma distribution. The better performance of the TPLR is consistent with the previous evaluations of transit time distributions in urban catchments where the engineered and more natural hydrological systems provide binary flow systems that are well estimated by two fast and slow flow reservoirs (Soulsby et al., 2014). The transit time models were unable to fully constrain the larger isotopic variability in the daily samples at the catchment outlet than the less frequently sampled sites upstream (Table 2). The limited variability in simulations relative to the measurements may be due to multiple factors. Heterogeneity in

precipitation may be highly pronounced in urban catchments, where cityscapes can alter the magnitude of summer storms, and variability in spatial patterns (Liu & Niyogi, 2019; Lorenz et al., 2019). This impacts volumetric inputs (potentially higher amounts between precipitation stations) and thereby isotopic compositions in recharge and runoff due to these through volumetric differences. This is supported by modelled data as peak flow and stream isotopes are under-estimated for the same events (e.g. 2019, Figures 4 and 5). Additional analysis of the sensitivity of spatio-temporal precipitation patterns and magnitudes may further help to improve model results. Further, stream isotope signature variability is affected by the sample resolution, where the outlet is near-daily and upstream sites are biweekly, which has been shown to influence model mixing and interpretation (Birkel et al., 2010). Finally, with increased downstream urbanization, the higher variability could be due to an exceedance of the sewer system threshold causing SWOs mixing within the stream (Quaranta et al., 2022). However, the influence of the SWO is dependent on the total SWO volume, stream discharge volume, infiltration within the SWO system (e.g. groundwater seepage; Rodriguez et al., 2020), tap water leakage, and the difference in isotopic composition of the SWO and stream discharge. In particular, the lower isotopic composition of groundwater as seepage contributions to SWO could lower the modelled isotopic composition of stream water towards those observed during the winter months when groundwater levels are the highest.

Water age evaluation within urban environments is complex due to significant changes to flow paths, engineered structures (e.g. drainage and diversions), water abstractions, and point load additions (WWTP). These numerous hydrologic changes directly influence the proportion of 'new' water (i.e. <2 months, Kirchner, 2016), which can further be divided into young 'new' water (e.g. precipitation) and young but 'older' recycled water (e.g. WWTP). The mixing approach provided an estimate of the separation of these water sources. In streams with no WWTP effluent, 16% of the natural flow was rainfall <2 months old. In streams with WWTP effluent, only 9% of flow was comprised of rainfall <2 months old. The estimates for stream flow inclusive of WWTP effluent were similar to young water fractions previously and independently estimated for all flow (6%, Marx et al. (2021)). These young 'new' water proportions, while relatively constrained within the mixing module, are slightly larger but more uncertain with the transit time models (12%–35%). Such young water fractions also carry unknown uncertainties of potential mixing of the direct flow component, which may be directly influenced by groundwater seepage and drinking water leakage into the SWO systems (e.g. Karpf & Krebs, 2013). Splitting young water (i.e. water entering the stream within the past 2 months) into 'new' (i.e. rainfall) and 'old' (i.e. WWTP) can have significant implications on interpretation. Within the Panke, 'older' young water (WWTP effluent) accounted for 41% of the total flow despite the new addition to the catchment which has a much more damped isotopic variability.

Interestingly, despite the relatively constrained discharge and water stable isotope simulations, the uncertainty in water ages was not well constrained for any of the isotopic modelling approaches (Figures 5 and 6); with differences between the semi-distributed

isotopic mixing and transit time approaches. While all isotopic modelling approaches showed decreasing water ages and transit times as percent urban cover increased - consistent with transit time studies in other urban environments (Soulsby et al., 2014, 2015) - and had moderate overlapping uncertainty bounds, the transit time models resulted in much younger average water age estimates (Table 4). However, the transit time distributions for young water (<200 days) are highly uncertain as the contributions of rapidly mobilized young water are not constrained by discharge estimations (as in the isotope mixing), which amplifies the larger uncertainty of the distribution tails already present within these approaches (Kirchner, 2016). Furthermore, there was more convergence of water age estimations with the choice of efficiency criteria used in calibration. Water ages for the different modelling approaches converged when either NSE or MAE were utilized, as both efficiency metrics penalized excessive simulated isotopic variability of younger water influence within the TTD models. For the isotope mixing module, the use of KGE resulted in much older water ages throughout the catchment (Table 4), which damped isotopic variability beyond the direct flow contributions of larger events. These results reveal the different sensitivity of the various efficiency criteria for model evaluation. This seems particularly apparent across model structures in urban environments where nonlinearities of flow contribution (e.g. SWOs), which if not adequately captured by the model structure, may result in overemphasis of incorrect flow paths.

4.3 | Limitations, wider implications and future work

The use of complementary modelling approaches within a learning framework to gain insights into the effect of urbanization on water fluxes and ages provided a more general opportunity to assess the wider implications of hydrological model conceptualizations - in particular, flow path and ecohydrology - within heavily urbanized systems. The continued development of urbanized areas, coupled with climatic change, places greater urgency on understanding these processes to evaluate long-term implications for urban water availability (Nguyen et al., 2010; Olsson et al., 2009).

While modelling studies within urban environments have a long history, much of the focus has been on the evaluation of urban storm drainage and flooding with relatively little focus on the differentiation of flow path contribution and water ages (Gillefalk et al., 2021). Concurrent discharge and isotopic datasets provided an opportunity to quantitatively understand the changes in flow path contribution from more rural to more urbanized regions of a catchment which provides further insight into the likely impact of future urbanization on fluxes (e.g. discharge, groundwater flow and evapotranspiration) (Soulsby et al., 2015). These coupled datasets proved to be invaluable within this study to spatially constrain model parameterization as required by the model structure (Feldman, 2000). While calibration provided spatial patterns of model parameters associated with differing degrees of urbanization regardless of sub-catchment size (Table S1), these patterns were calibration-dependent and the transferability to other

catchments may be limited. Further, the significant influence of the WWTP effluent and weir diversion (Pase) likely influenced the parameterization, and further work is needed to evaluate how flow management affects hydrological parameterization. While the evapotranspiration estimated from the model was within previous estimates, the overall estimate was still low causing some overestimation of discharge. The implementation of evapotranspiration estimates as forcing data has been shown to have the potential to improve model discharge performance (Zare et al., 2021) and could help further constrain source water estimations, particularly in natural groundwater dominated environments like the study area (Smith et al., 2021). Gridded input of evapotranspiration could further help to limit spatial biasing at the sub-catchment scale in lumped modelled caused by reduced heterogeneity influences (Salvadore et al., 2015).

While the simpler hydrological structure approach reduced parameterization compared to a more physically based or fully distributed modelling approach, this ultimately compromised the isotopic modelling. The use of physically based modelling can result in no additional parameterization needs for tracer mixing (e.g. Ech_2O -iso, Kuppel et al., 2018), which reduces uncertainty over flow path representation and mixing simultaneously without increasing degrees of freedom. While the isotopic mixing module used provided insight to total mixing volumes, the additional parameterization and use of calibrated hydrological results reduced the emphasis on flow path identification and was likely the main reason for the higher water age uncertainty. The uncertainty of the more simple transit time models was more predictable given the already well-known problem of capturing large uncertainties of complex flow processes in urban environments using black-box models (Bonneau et al., 2017). In particular, convective precipitation cells which produce high-intensity rainfall, and are important in summer, can cause non-linearities in the quantity of stormwater reaching the streams (e.g. Launay et al., 2016) which directly influences how well more simple models running on a 12 h time step can capture complex flow, dynamic responses.

5 | CONCLUSION

We utilized a distributed rainfall-runoff model with an isotope mixing model as a learning framework to better understand the hydrology of a complex 217 km² heavily urbanized catchment in Berlin, Germany. The approaches focused on evaluating flow paths and water ages while optimizing the information content from available datasets and reducing parameterization, with both coupled semi-distributed hydrological tracer mixing, and evaluation of stream water transit times throughout the catchment. Upstream headwater catchments with less urbanization showed very high groundwater contribution to streamflow, important for sustaining baseflows during the drier summer months. Lower summer baseflow resulted in the more pronounced influence of direct runoff from impervious surfaces during convective precipitation events. Wastewater effluent contributions dominated streamwater downstream of a major wastewater treatment plant, though with a decreased influence of effluent and direct urban runoff

after a stream weir diversion. Water ages in stream water showed a notable decrease downstream in the catchment as the proportion of urban area increased. Younger, more rapid water contributions were the driving forces behind downstream isotopic variability despite limited discharge variability due to the wastewater treatment effluent and flow diversion. Utilizing simple tracer-aided models within a learning framework can help to provide a further understanding of urban catchment hydrology through the lens of water ages while aiding in the identification of the spatio-temporal variation in dominant processes that are unique to urban environments. The approach taken within this study provides a stepping stone to further hydrological and ecohydrological exploration within urban landscapes.

ACKNOWLEDGEMENTS

We acknowledge the BMBF (funding code 033W034A) which supported the stable isotope laboratory at IGB. Funding for DT was also received through the Einstein Research Unit 'Climate and Water under Change' from the Einstein Foundation Berlin and Berlin University Alliance. We acknowledge funding from the graduate School Urban Water financed by Interfaces Deutsche Forschungsgemeinschaft, Grant/Award Number: (GRK2032/2). CS is also funded by the ISOLAND Project of the Leverhulme Trust, Grant Number: (RPG-2018-425). CM and CS are funded for the project MOSAIC by the Einstein Stiftung Berlin, Grant/Award Number: EVF-2018-425. The authors would like to thank the two anonymous reviewers and editor (Jim McNamara) for the comments and feedback which has improved the manuscript. Open Access funding enabled and organized by Projekt DEAL.

DATA AVAILABILITY STATEMENT

The data that support the findings of this study are available on request from the corresponding author. The data are not publicly available due to privacy or ethical restrictions.

ORCID

Christian Marx  <https://orcid.org/0000-0001-7648-1603>

Chris Soulsby  <https://orcid.org/0000-0001-6910-2118>

REFERENCES

- Ala-Aho, P., Tetzlaff, D., McNamara, J. P., Laudon, H., & Soulsby, C. (2017). Using isotopes to constrain water flux and age estimates in snow-influenced catchments using the STARR (spatially distributed tracer-aided rainfall-runoff) model. *Hydrology and Earth System Sciences*, 21(10), 5089–5110. <https://doi.org/10.5194/hess-21-5089-2017>
- Allen, R. G., Pereira, L. S., Raes, D., & Smith, M. (1998). Crop evapotranspiration—guidelines for computing crop water requirements. *FAO Irrigation and Drainage Paper (FAO)* (56): 300p.
- Bednorz, F., & Brose, D. (2017). Altersdatierung mittels Isotopenanalytik zur Verweilzeitbestimmung und Identifizierung von Speisungsanteilen des Grundwassers in Brandenburg. *Brandenburgische Geowissenschaftliche Beiträge*, 19, 83–101.
- Bennett, T., & Peters, J. (2000). Continuous soil moisture accounting in the hydrologic engineering center hydrologic modeling system (HEC-HMS). *Building Partnerships*, 1–10. [https://doi.org/10.1061/40517\(2000\)149](https://doi.org/10.1061/40517(2000)149)
- Berthier, E., Andrieu, H., & Creutin, J. D. (2004). The role of soil in the generation of urban runoff: Development and evaluation of a 2D model. *Journal of Hydrology*, 299(3–4), 252–266. <https://doi.org/10.1016/j.jhydrol.2004.08.008>
- Beven, K., & Binley, A. (1992). The future of distributed models: Model calibration and uncertainty prediction. *Hydrological Processes*, 6(3), 279–298. <https://doi.org/10.1002/hyp.3360060305>
- Birkel, C., Dunn, S. M., Tetzlaff, D., & Soulsby, C. (2010). Assessing the value of high-resolution isotope tracer data in the stepwise development of a lumped conceptual rainfall-runoff model. *Hydrological Processes*, 24(16), 2335–2348. <https://doi.org/10.1002/hyp.7763>
- Birkel, C., Tetzlaff, D., Dunn, S. M., & Soulsby, C. (2011). Using time domain and geographic source tracers to conceptualize streamflow generation processes in lumped rainfall-runoff models. *Water Resources Research*, 47(2), 1–15. <https://doi.org/10.1029/2010WR009547>
- Bonneau, J., Fletcher, T. D., Costelloe, J. F., & Burns, M. J. (2017). Stormwater infiltration and the 'urban karst' – A review. *Journal of Hydrology*, 552, 141–150. <https://doi.org/10.1016/j.jhydrol.2017.06.043>
- Cammaleri, C., Naumann, G., Mentaschi, L., Bisselink, B., Gelati, E., Roo, A., & Feyen, L. (2020). Diverging hydrological drought traits over Europe with global warming. *Hydrology and Earth System Sciences*, 24, 5919–5935. <https://doi.org/10.5194/hess-24-5919-2020>
- Cunge, J. A. (1969). On the subject of a flood propagation computation method (Muskingum method). *Journal of Hydraulic Research*, 7(2), 205–230.
- D'Errico, J. (2022). Fminsearchbnd. MATLAB Central File Exchange. <https://www.mathworks.com/matlabcentral/fileexchange/8277-fminsearchbnd-fminsearchcon>
- Duarte Rocha, A., Vulova, S., van der Tol, C., Förster, M., & Kleinschmit, B. (2022). Modelling hourly evapotranspiration in urban environments with SCOPE using open remote sensing and meteorological data. *Hydrology and Earth System Sciences*, 26, 1111–1129. <https://doi.org/10.5194/hess-26-1111-2022>
- DWD. (2022). CDC (Climate Data Center). https://www.dwd.de/DE/klimaumwelt/cdc/cdc_node.html;jsessionid=A28B6A63B4B7E4DCB78444CD24A3CDD8.live31094
- Ehleringer, J. R., Barnette, J. E., Jameel, Y., Tipple, B. J., & Bowen, G. J. (2016). Urban water – A new frontier in isotope hydrology†. *Isotopes in Environmental and Health Studies*, 52(4–5), 477–486. <https://doi.org/10.1080/10256016.2016.1171217>
- European Environment Agency. (2014). Water use in Europe – quantity and quality face big challenges. <https://www.eea.europa.eu/signals/signals-2018-content-list/articles/water-use-in-europe-2014>
- Feldman, A. (2000). Hydrologic modeling system technical reference manual. In *Hydrologic modeling system HEC-HMS technical reference manual (March)* (p. 148). U.S. Army Corps of Engineers.
- Fidal, J., & Kjeldsen, T. R. (2020). Accounting for soil moisture in rainfall-runoff modelling of urban areas. *Journal of Hydrology*, 589, 125122. <https://doi.org/10.1016/j.jhydrol.2020.125122>
- Fletcher, T. D., Andrieu, H., & Hamel, P. (2013). Understanding, management and modelling of urban hydrology and its consequences for receiving waters: A state of the art. *Advances in Water Resources*, 51, 261–279. <https://doi.org/10.1016/j.advwatres.2012.09.001>
- Frick, M., Scheck-Wenderoth, M., Schneider, M., & Cacace, M. (2019). Surface to groundwater interactions beneath the City of Berlin: Results from 3D models. *Geofluids*, 2019, 1–22. <https://doi.org/10.1155/2019/4129016>
- Gillefalk, M., Tetzlaff, D., Hinkelmann, R., Kuhlemann, L. M., Smith, A., Meier, F., Maneta, M. P., & Soulsby, C. (2021). Quantifying the effects of urban green space on water partitioning and ages using an isotope-based ecohydrological model. *Hydrology and Earth System Sciences*, 25(6), 3635–3652. <https://doi.org/10.5194/hess-25-3635-2021>
- Gillefalk, M., Tetzlaff, D., Marx, C., Smith, A., Meier, F., Hinkelmann, R., & Soulsby, C. (2022). Estimates of water partitioning in complex urban landscapes with isotope-aided ecohydrological modelling. *Hydrological Processes*, 36, e14532. <https://doi.org/10.1002/hyp.14532>

- Godsey, S. E., Aas, W., Clair, T. A., de Wit, H. A., Fernandez, I. J., Kahl, J. S., Malcolm, I. A., Neal, C., Neal, M., Nelson, S. J., Norton, S. A., Palucis, M. C., Skjelkvåle, B. L., Soulsby, C., Tetzlaff, D., & Kirchner, J.W. (2010). Generality of fractal 1/f scaling in catchment tracer time series, and its implications for catchment travel time distributions. *Hydrological Processes*, 24, 1660–1671. <https://doi.org/10.1002/hyp.7677>
- Gudmundsson, L., & Seneviratne, S. I. (2016). Anthropogenic climate change affects meteorological drought risk in Europe. *Environmental Research Letters*, 11(4), 44005.
- Gupta, H. V., Kling, H., Yilmaz drought, K. K., & Martinez, G. F. (2009). Decomposition of the mean squared error and NSE performance criteria: Implications for improving hydrological modelling. *Journal of Hydrology*, 377(1), 80–91. <https://doi.org/10.1016/j.jhydrol.2009.08.003>
- Güneralp, B., Güneralp, I., & Liu, Y. (2015). Changing global patterns of urban exposure to flood and hazards. *Global Environmental Change*, 31, 217–225. <https://doi.org/10.1016/j.gloenvcha.2015.01.002>
- Hersbach, H., Bell, B., Berrisford, P., Biavati, G., Horányi, A., Muñoz Sabater, J., Nicolas, J., Peubey, C., Radu, R., Rozum, & I., et al. (2019). ERA5 monthly averaged data on single levels from 1979 to present. Copernicus Climate Change Service (C3S) Climate Data Store (CDS). <https://doi.org/10.24381/cds.f17050d7>
- Huang, S., Krysanova, V., & Hattermann, F. F. (2013). Projection of low flow conditions in Germany under climate change by combining three RCMs and a regional hydrological model. *Acta Geophysica*, 61(1), 151–193. <https://doi.org/10.1024/s11600-012-0065-1>
- Huang, S., Krysanova, V., & Hattermann, F. F. (2015). Projections of climate change impacts on floods and droughts in Germany using an ensemble of climate change scenarios. *Regional Environmental Change*, 15, 461–473. <https://doi.org/10.1007/s10113-014-0606-z>
- Ichiba, A., Gires, A., Tchiguirinskaia, I., Schertzer, D., Bompard, P., & Ten, V. M. C. (2018). Scale effect challenges in urban hydrology highlighted with a distributed hydrological model. *Hydrology and Earth System Sciences*, 22(1), 331–350. <https://doi.org/10.5194/hess-22-331-2018>
- Inamdar, S., Dhillon, G., Singh, S., Dutta, S., Levia, D., Scott, D., Mitchell, M., Van Stan, J., & McHale, P. (2013). Temporal variation in end-member chemistry and its influence on runoff mixing patterns in a forested piedmont catchment. *Water Resources Research*, 49(4), 1828–1844. <https://doi.org/10.1002/wrcr.20158>
- Karpp, C., & Krebs, P. (2013). Modelling of groundwater infiltration into sewer systems. *Urban Water Journal*, 10(4), 221–229. <https://doi.org/10.1080/1573062X.2012.724077>
- Kirchner, J. W. (2016). Aggregation in environmental systems-part 1: Seasonal tracer cycles quantify young water fractions, but not mean transit times, in spatially heterogeneous catchments. *Hydrology and Earth System Sciences*, 20(1), 279–297. <https://doi.org/10.5194/hess-20-279-2016>
- Kleine, L., Tetzlaff, D., Smith, A., Wang, H., & Soulsby, C. (2020). Using water stable isotopes to understand evaporation, moisture stress, and re-wetting in catchment forest and grassland soils of the summer drought of 2018. *Hydrology and Earth System Sciences*, 24(7), 3737–3752. <https://doi.org/10.5194/hess-24-3737-2020>
- Kuhlemann, L. M., Tetzlaff, D., & Soulsby, C. (2020). Urban water systems under climate stress: An isotopic perspective from Berlin. *Germany. Hydrological Processes*, 34(18), 3758–3776. <https://doi.org/10.1002/hyp.13850>
- Kuhlemann, L. M., Tetzlaff, D., Smith, A., Kleinschmit, B., & Soulsby, C. (2021). Using soil water isotopes to infer the influence of contrasting urban green space on ecohydrological partitioning. *Hydrology and Earth System Sciences*, 25(2), 927–943. <https://doi.org/10.5194/hess-25-927-2021>
- Kuppel, S., Tetzlaff, D., Maneta, M. P., & Soulsby, C. (2018). Ech2O-iso 1.0: Water isotopes and age tracking in a process-based, distributed ecohydrological model. *Geoscientific Model Development*, 11(7), 3045–3069. <https://doi.org/10.5194/gmd-11-3045-2018>
- Kuppel, S., Tetzlaff, D., Maneta, M., & Soulsby, C. (2020). Critical zone storage controls on the water ages of ecohydrological outputs. *Geophysical Research Letters*, 47, e2020GL088897. <https://doi.org/10.1029/2020GL088897>
- Lagarias, J. C., Reeds, J. A., Wright, M. H., & Wright, P. E. (1998). Convergence properties of the Nelder–Mead simplex method in low dimensions. *SIAM Journal on Optimization*, 9(1), 112–147. <https://doi.org/10.1137/S1052623496303470>
- Launay, M. A., Dittmer, U., & Steinmetz, H. (2016). Organic micropollutants discharged by combined sewer overflows – characterisation of pollutant sources and stormwater-related processes. *Water Research*, 104, 82–92. <https://doi.org/10.1016/j.watres.2016.07.068>
- Limberg, A., & Thierbach, J. (2002). Hydrostratigrafie von Berlin–Korrelation mit dem Norddeutschen Gliederungsschema. *Brandenburgische Geowissenschaftliche Beiträge*, 9(1/2), 65–68.
- Liu, J., & Niyogi, D. (2019). Meta-analysis of urbanization impact on rainfall modification. *Scientific Reports*, 9, 7301. <https://doi.org/10.1038/s41598-019-42494-2>
- Lorenz, J. M., Kronenberg, R., Bernhofer, C., & Niyogi, D. (2019). Urban rainfall modification: Observational climatology over Berlin, Germany. *Journal of Geophysical Research: Atmospheres*, 124, 731–746. <https://doi.org/10.1029/2018JD028858>
- Marx, C., Tetzlaff, D., Hinkelmann, R., & Soulsby, C. (2021). Isotope hydrology and water sources in a heavily urbanized stream. *Hydrological Processes*, 35(10), 1–20. <https://doi.org/10.1002/hyp.14377>
- Massmann, G., Pekdeger, A., Heberer, T., Grützmacher, G., Dünnbier, U., Knappe, A., Meyer, H., & Mechlinski, A. (2007). Drinking-water production in urban environments—Bank filtration in Berlin. *Grundwasser*, 12(3), 232–245. <https://doi.org/10.1007/s00767-007-0036-7>
- McGrane, S. J. (2016). Impacts of urbanisation on hydrological and water quality dynamics, and urban water management: A review. *Hydrological Sciences Journal*, 61(13), 2295–2311. <https://doi.org/10.1080/02626667.2015.1128084>
- Meierdiecks, K. L., Smith, J. A., Baeck, M. L., & Miller, A. J. (2010). Heterogeneity of hydrologic response in urban watersheds. *JAWRA Journal of the American Water Resources Association*, 46, 1221–1237. <https://doi.org/10.1111/j.1752-1688.2010.00487.x>
- Meili, N., Manoli, G., Burlando, P., Bou-Zeid, E., Chow, W. T. L., Coutts, A. M., Daly, E., Nice, K. A., Roth, M., Tapper, N. J., Velasco, E., Vivoni, E. R., & Fatichi, S. (2020). An urban ecohydrological model to quantify the effect of vegetation on urban climate and hydrology (UT&C v1.0). *Geoscientific Model Development*, 13(1), 335–362. <https://doi.org/10.5194/gmd-13-335-2020>
- Monteith, J. (1965). Evaporation and environment. *Symposia of the Society for Experimental Biology*, 19, 205–234.
- Nash, J. E., & Sutcliffe, J. V. (1970). River flow forecasting through conceptual models part I - a discussion of principles. *Journal of Hydrology*, 10(3), 282–290. [https://doi.org/10.1016/0022-1694\(70\)90255-6](https://doi.org/10.1016/0022-1694(70)90255-6)
- Nguyen, V. T., Desramaut, N., & Nguyen, T. D. (2010). Optimal rainfall temporal patterns for urban drainage design in the context of climate change. *Water Science and Technology: A Journal of the International Association on Water Pollution Research*, 62(5), 1170–1176.
- Olsson, J., Berggren, K., Olofsson, M., & Viklander, M. (2009). Applying climate model precipitation scenarios for urban hydrological assessment: A case study in Kalmar City, Sweden. *Atmospheric Research*, 92, 364–375. <https://doi.org/10.1016/j.atmosres.2009.01.015>
- Page, T., Smith, P., Beven, K., Pianosi, F., Sarrazin, F., Almeida, S., Holcome, L., Freer, J., & Wagener, T. (2022). The CURE Uncertainty Estimation Toolbox. http://www.uncertain-future.org.uk/?page_id=26
- Pang, X., Gu, Y., Launiainen, S., & Guan, M. (2022). Urban hydrological responses to climate change and urbanization in cold climates. *Science*

- of the *Total Environment*, 817, 153066. <https://doi.org/10.1016/j.scitotenv.2022.153066>
- Perret, E., Renard, B., & Le Coz, J. (2020). A rating curve model accounting for cyclic stage-discharge shifts due to seasonal aquatic vegetation. *Water Resources Research*, 57, e2020WR027745. <https://doi.org/10.1029/2020WR027745>
- Petrucci, G., & Bonhomme, C. (2014). The dilemma of spatial representation for urban hydrology semi-distributed modelling: Trade-offs among complexity, calibration and geographical data. *Journal of Hydrology*, 517, 997–1007. <https://doi.org/10.1016/j.jhydrol.2014.06.019>
- Quaranta, E., Fuchs, S., Liefting, H., Schellart, A., & Pistocchi, A. (2022). A hydrological model to estimate pollution from combined sewer overflows at the regional scale: Application to Europe. *Journal of Hydrology: Regional Studies*, 41, 101080. <https://doi.org/10.1016/j.ejrh.2022.101080>
- Rodriguez, F., Le Delliou, A.-L., Andrieu, H., & Gironas, J. (2020). Groundwater contribution to sewer network baseflow in an urban catchment-case study of pin sec catchment, Nantes, France. *Water*, 12, 3. <https://doi.org/10.3390/w12030689>
- Salvadore, E., Bronders, J., & Batelaan, O. (2015). Hydrological modelling of urbanized catchments: A review and future directions. *Journal of Hydrology*, 529(P1), 62–81. <https://doi.org/10.1016/j.jhydrol.2015.06.028>
- Scharffenberg, W., & Fleming, M. (2008). Hydrologic modeling system user's manual. Transform (September): 290.
- Senate Department for the Environment T and CP (SenUVK). (2021). Wasserportal Gewässerkundliche Messdaten. wasserportal.berlin.de
- Senate Department for Urban Development and the Environment. (2012). Morphology of water bodies—Overall assessment (WRRL), p. 7.
- Sikorska, A. E., Scheidegger, A., Banasik, K., & Rieckermann, J. (2013). Considering rating curve uncertainty in water level predictions. *Hydrology and Earth System Sciences*, 17, 4415–4427. <https://doi.org/10.5194/hess-17-4415-2013>
- Singh, J., Karmakar, S., PaiMazumder, D., Ghosh, S., & Niyogi, D. (2020). Urbanization alters rainfall extremes over the contiguous United States. *Environmental Research Letters*, 15(7), 74033.
- Smith, A., Tetzlaff, D., Gelbrecht, J., Kleine, L., & Soulsby, C. (2020). Riparian wetland rehabilitation and beaver re-colonization impacts on hydrological processes and water quality in a lowland agricultural catchment. *Science of the Total Environment*, 699(9), 134302. <https://doi.org/10.1016/j.scitotenv.2019.134302>
- Smith, A., Tetzlaff, D., Kleine, L., Maneta, M. P., & Soulsby, C. (2020). Isotope-aided modelling of ecohydrologic fluxes and water ages under mixed land use in Central Europe: The 2018 drought and its recovery. *Hydrological Processes*, 34(16), 3406–3425. <https://doi.org/10.1002/hyp.13838>
- Smith, A., Tetzlaff, D., Kleine, L., Maneta, M., & Soulsby, C. (2021). Quantifying the effects of land use and model scale on water partitioning and water ages using tracer-aided ecohydrological models. *Hydrology and Earth System Sciences*, 25(4), 2239–2259. <https://doi.org/10.5194/hess-25-2239-2021>
- Soulsby, C., Birkel, C., & Tetzlaff, D. (2014). Assessing urbanization impacts on catchment transit times. *Geophysical Research Letters*, 41, 442–448. <https://doi.org/10.1002/2013GL058716>
- Soulsby, C., Birkel, C., Geris, J., & Tetzlaff, D. (2015). Spatial aggregation of time-variant stream water ages in urbanizing catchments. *Hydrological Processes*, 29(13), 3038–3050. <https://doi.org/10.1002/hyp.10500>
- Tetzlaff, D., Piovano, T., Ala-Aho, P., Smith, A., Carey, S. K., Marsh, P., Wookey, P., Street, L., & Soulsby, C. (2018). Using stable isotopes to estimate travel times in a data-sparse Arctic catchment: Challenges and possible solutions. *Hydrological Processes*, 32(12), 1936–1952. <https://doi.org/10.1002/hyp.13146>
- Turner, S. W. D., Rice, J. S., Nelson, K. D., Vernon, C. R., McManamay, R., Dickson, K., & Marston, L. (2021). Comparison of potential drinking water source contamination across one hundred U.S. cities. *Nature Communications*, 12(1), 1–12. <https://doi.org/10.1038/s41467-021-27509-9>
- United Nations. (2018). *World urbanization prospects: The 2018 revision*. United Nations.
- Westerberg, I. K., & McMillan, H. K. (2015). Uncertainty in hydrological signatures. *Hydrology and Earth System Sciences*, 19, 3951–3968. <https://doi.org/10.5194/hess-19-3951-2015>
- Wu, S., Tetzlaff, D., Yang, X., & Soulsby, C. (2022). Disentangling the influence of landscape characteristics, hydroclimatic variability and land management on surface water NO₃-N dynamics: Spatially distributed modeling over 30 yr in a lowland mixed land use catchment. *Water Resources Research*, 58(2), e2021WR030566. <https://doi.org/10.1029/2021wr030566>
- Yang, L., Ni, G., Tian, F., & Niyogi, D. (2021). Urbanization exacerbated rainfall over European suburbs under a warming climate. *Geophysical Research Letters*, 48(21), e2021GL095987. <https://doi.org/10.1029/2021GL095987>
- Zare, M., Pakparvar, M., Jamshidi, S., Bazrafshan, O., & Ghahari, G. (2021). Optimizing the runoff estimation with HEC-HMS model using spatial evapotranspiration by the SEBS model. *Water Resources Management*, 35(8), 2633–2648. <https://doi.org/10.1007/s11269-021-02855-x>

SUPPORTING INFORMATION

Additional supporting information can be found online in the Supporting Information section at the end of this article.

How to cite this article: Smith, A., Tetzlaff, D., Marx, C., & Soulsby, C. (2023). Enhancing urban runoff modelling using water stable isotopes and ages in complex catchments. *Hydrological Processes*, 37(2), e14814. <https://doi.org/10.1002/hyp.14814>